

POLARISED ELECTROMAGNETIC WAVE  
PROPAGATION THROUGH THE FERROMAGNET:  
PHASE BOUNDARY OF DYNAMIC PHASE  
TRANSITION

MUKTISH ACHARYYA

Department of Physics, Presidency University  
86/1 College Street, Calcutta-700073, India  
muktish.physics@presiuniv.ac.in

*(Received January 7, 2014; revised version received January 23, 2014;  
final version received February 10, 2014)*

The dynamical responses of ferromagnet to the propagating electromagnetic field wave passing through it are modelled and studied here by Monte Carlo simulation in the two-dimensional Ising model. Here, the electromagnetic wave is linearly polarised in such a way that the direction of magnetic field is parallel to that of the magnetic spins. The coherent spin-cluster propagating mode is observed. The time average magnetisation over the full cycle (time) of the field defines the order parameter of the dynamic phase transition. Depending on the value of the temperature and the amplitude of the propagating magnetic field wave, a dynamical phase transition is observed. The transition is detected by studying the temperature dependences of the variance of the dynamic order parameter, the derivative of the dynamic order parameter and the dynamic specific heat. The phase boundary of the dynamic transitions are drawn for two different values of the wave length of the propagating magnetic field wave. The phase boundary is observed to shrink (inward) for shorter wavelength of the EM wave. The signature of the divergence of the relevant length scale is observed at the transition point.

DOI:10.5506/APhysPolB.45.1027

PACS numbers: 05.50.+q, 05.70.Ln, 75.30.Ds, 75.30.Kz

## 1. Introduction

The dynamical response of Ising ferromagnet to a time dependent magnetic field has become an active field of research [1]. The hysteretic responses and the nonequilibrium dynamic phase transitions are two main points of

attention. The scaling behaviour [2] of hysteresis loop area with the amplitude, frequency of the sinusoidally oscillating magnetic field is the main outcome of the research. Another interesting aspect is the nonequilibrium dynamic phase transition which has produced variety of interesting results and prompted the researchers to take continuous attention in this field. Historically, some important observations like (i) divergences of dynamic specific heat and relaxation time near the transition point [3], (ii) divergence of the relevant length-scale near the transition point [4], (iii) studies regarding the existence of tricritical point [5, 6], (iv) the relation with the stochastic resonance [5] and the hysteretic loss [7] enriched the field and established that the dynamic transition has similarity to the well-known equilibrium thermodynamic phase transition. Very recently, a surface dynamic phase transition [8] has been observed in the kinetic Ising ferromagnet driven by oscillating magnetic field. The dynamic phase transition was detected also experimentally [9] in the ultrathin Co film on Cu(001) system by surface magneto-optic Kerr effect. The direct excitation of propagating spin waves by focused ultrashort optical pulses have been recently investigated [10]. The transient behaviour of the dynamically ordered phase in uniaxial cobalt film is also studied experimentally [11].

This dynamic phase transition is also observed in other magnetic models. The off-axial dynamic phase transition was observed [12] in the anisotropic classical Heisenberg model and in the XY model [13]. The multiple (surface and bulk) dynamic transition was observed [14] in the classical Heisenberg model. The multiple dynamic transition was found [15] also in the Heisenberg ferromagnet driven by polarised magnetic field. The dynamic transition was observed [16] in the kinetic spin-3/2 Blume–Capel model and in the Blume–Emery–Griffith model [17] by meanfield calculations. The dynamic phase transition was studied by the Monte Carlo simulation [18] and meanfield calculation [19] in the Ising metamagnet.

It may be noted here, that all the studies mentioned so far, were done by sinusoidally oscillating magnetic field which was uniform over the space (lattice) at any instant of time. In those studies, the spatio-temporal variation of applied magnetic field was not considered. One such spatio-temporal variation of applied magnetic field would be the propagating magnetic field wave. In reality, if the electromagnetic wave passes through the ferromagnet, the varying (with space and time) magnetic field coupled with the spin, will affect the dynamic nature of the system. Here, also dynamic transition will be observed. Very recently, it has been briefly reported [20] that propagating magnetic field wave would lead to a dynamical phase transition in the Ising ferromagnet. A pinned phase and a phase of coherent motion of spin-clusters were observed recently [21] in the random field Ising model, swept by propagating magnetic field wave. Here, the nonequilibrium dynamic phase transition is *athermal* and tuned by quenched random (field)

disorder. A rich dynamical phase boundary (with four different phases) was also drawn. A dynamic symmetry breaking breathing and spreading transitions [22] were also recently found in a ferromagnetic film irradiated by the spherical electromagnetic wave.

In this paper, the nonequilibrium dynamic phase transition is studied extensively in the two-dimensional Ising ferromagnet swept by polarised propagating electromagnetic field wave with the Monte Carlo (MC) simulation and the phase boundary of the dynamical phase transition is drawn. The paper is organised as follows: The model and the MC simulation technique are discussed in Sec. 2, the numerical results are reported in Sec. 3 and the paper ends with a summary, in Sec. 4.

## 2. Model and simulation

The Hamiltonian (time dependent) representing the two-dimensional Ising ferromagnet (having uniform nearest neighbour interaction) in presence of a polarised propagating electromagnetic field wave (having spatio-temporal variation) can be written as

$$H(t) = -J \sum s(x, y, t) s(x', y', t) - \Sigma h(x, y, t) s(x, y, t). \quad (1)$$

The  $s(x, y, t)$  represents the Ising spin variable ( $\pm 1$ ) at lattice site  $(x, y)$  at time  $t$  on a square lattice of linear size  $L$ .  $J (> 0)$  is the ferromagnetic (taken here as uniform) interaction strength. The summation in the first term represents the Ising spin-spin interaction and is carried over the nearest neighbours only. The  $h(x, y, t)$  is the value of the magnetic field (at point  $(x, y)$  and at any time  $t$ ) of the propagating electromagnetic wave. It may be noted here that the electromagnetic wave is linearly polarised in such a way that the direction of magnetic field is parallel to that of the spins. For a propagating magnetic field, wave  $h(x, y, t)$  takes the form

$$h(x, y, t) = h_0 \cos(2\pi ft - 2\pi y/\lambda). \quad (2)$$

The  $h_0$ ,  $f$  and  $\lambda$  represent the amplitude, frequency and the wavelength, respectively, of the propagating electromagnetic field wave which propagates along the  $y$ -direction. In the present simulation, an  $L \times L$  square lattice is considered. The boundary condition, used here, is periodic in both the  $(x$  and  $y)$  directions. The initial ( $t = 0$ ) configuration is chosen as the half of the total number (selected randomly) of spins are up ( $s(x, y, t = 0) = +1$ ). This configuration of spins corresponds to the high temperature disordered phase. The spins are updated randomly (a site  $(x, y)$  is chosen at random) and spin flip occurs (at temperature  $T$ ) according to the Metropolis rate ( $W$ ) [23]

$$W(s \rightarrow -s) = \text{Min}[\exp(-\Delta E/k_B T), 1], \quad (3)$$

where  $\Delta E$  is the change in energy due to the spin flip and  $k_B$  is the Boltzmann constant.  $L^2$  such random updates of spins constitutes the unit time step here and is called the Monte Carlo step per spin (MCSS). Here, the value of magnetic field is measured in the unit of  $J$  and the temperature is measured in the unit of  $J/k_B$ . The dynamical steady state is reached by cooling the system slowly in small steps ( $\delta T = 0.02$  here) of temperature, from the high temperature, dynamically disordered configuration. This particular choice is a compromise between the computational time and the precision in measuring the transition temperature. The frequency of the propagating magnetic field wave was taken  $f = 0.01$  throughout the study. The total length of the simulation is  $2 \times 10^5$  MCSS and first  $10^5$  MCSS transient data were discarded. The data are taken by averaging over  $10^5$  MCSS. In some cases, near the transition points, averaging was done over  $2 \times 10^5$  MCSS, after discarding initial  $2 \times 10^5$  MCSS. Since the frequency of the propagating field is  $f = 0.01$ , the complete cycle of the field requires 100 MCSS. So, in  $10^5$  MCSS,  $10^3$  numbers of cycles of the propagating field are present. The time averaged data over the full cycle (100 MCSS) of the propagating field are further averaged over 1000 cycles.

### 3. Results

In this study, a square lattice of size  $L = 100$  is considered. The steady state dynamical behaviours of the spins are studied here. The amplitude, frequency and the wavelength of the propagating wave are taken  $h_0 = 0.6$ ,  $f = 0.01$  and  $\lambda = 25$  respectively. The magnetic field is propagating along the  $y$ -direction (vertically upward in the graphs). The temperature of the system is taken  $T = 1.50$ . The configuration of the spins, at any instant of time  $t = 100100$  MCS, are shown in Fig. 1 (a). Here, it is noted that the clusters of spins are formed in strips and these strips move coherently as time goes on. The propagation of the spin-strips are clear in Fig. 1 (b), where the snapshot was taken at instant  $t = 100125$  MCSS. The similar study is performed at a lower temperature  $T = 1.26$  (with all other parameters of the propagating field remain same). Here, the spin clusters are observed to be formed in such shapes which are not like the strips (as observed in the case of higher temperature  $T = 1.50$ , mentioned above). This is shown in Fig. 1 (c), at any instant  $t = 100100$  MCSS. These irregularly shaped spin-clusters are observed to propagate (along the direction of propagating magnetic field), which is clear from Fig. 1 (d) (for  $t = 100125$  MCSS).

To show the propagations of these spin-clusters, the instantaneous line magnetisation  $m(y, t) = (\int s(x, y, t) dx / L)$  was plotted against  $y$  at any particular instant  $t = 100100$  MCSS. This is shown in Fig. 2 (a) (compare with Fig. 1 (a)). The periodic variation of  $m(y, t)$  along  $y$ -direction is found. This was observed to propagate, see Fig. 2 (b) and compare with Fig. 1 (b) when

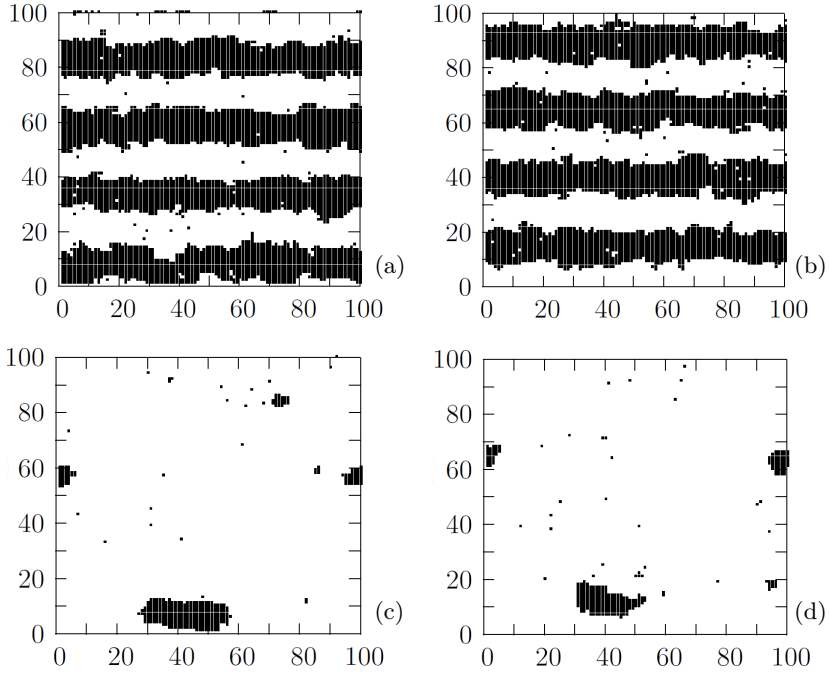


Fig. 1. The motion of spin-clusters of down spins (shown by black dots), swept by propagating magnetic field wave, for different values of (a)  $t = 100100$  MCSS,  $T = 1.5$  and  $h_0 = 0.6$ , (b)  $t = 100125$  MCSS,  $T = 1.5$  and  $h_0 = 0.6$ , (c)  $t = 100100$  MCSS,  $T = 1.26$  and  $h_0 = 0.6$ , (d)  $t = 100125$  MCSS,  $T = 1.26$  and  $h_0 = 0.6$ .

shown at different time  $t = 100125$  MCSS. It may be noted here that the line magnetisation is periodic (with  $y$ ) at any instant of time  $t$ . This is also periodic in time  $t$  at any position  $y$ . The oscillation is symmetric about  $m(y) = 0$  line (for higher temperature  $T = 1.50$ ). Here, the time average magnetisation over a full cycle of the propagating field is  $Q = \frac{f}{L} \int \int m(y, t) dy dt$  and becomes zero (due to symmetric oscillation about  $m(y) = 0$  line). This corresponds to a dynamically symmetric phase.

Now, for lower temperature  $T = 1.26$ , the spatio-temporal periodicity of the line magnetisation is lost. The symmetric-oscillation (about  $m(y) = 0$  line) is lost here. This corresponds to a dynamically symmetry-broken phase. As a consequence, the time averaged magnetisation over a full cycle of the propagating field becomes nonzero. These are shown in Fig. 2 (c) and Fig. 2 (d) (may be compared with Fig. 1 (c) and Fig. 1 (d), respectively). However, in this case the spin-clusters were observed to propagate. So, as the temperature decreases,  $Q$  becomes nonzero (lower temperature) from a zero value (higher temperature). This  $Q$  defines the order parameter of the dynamic phase transition.

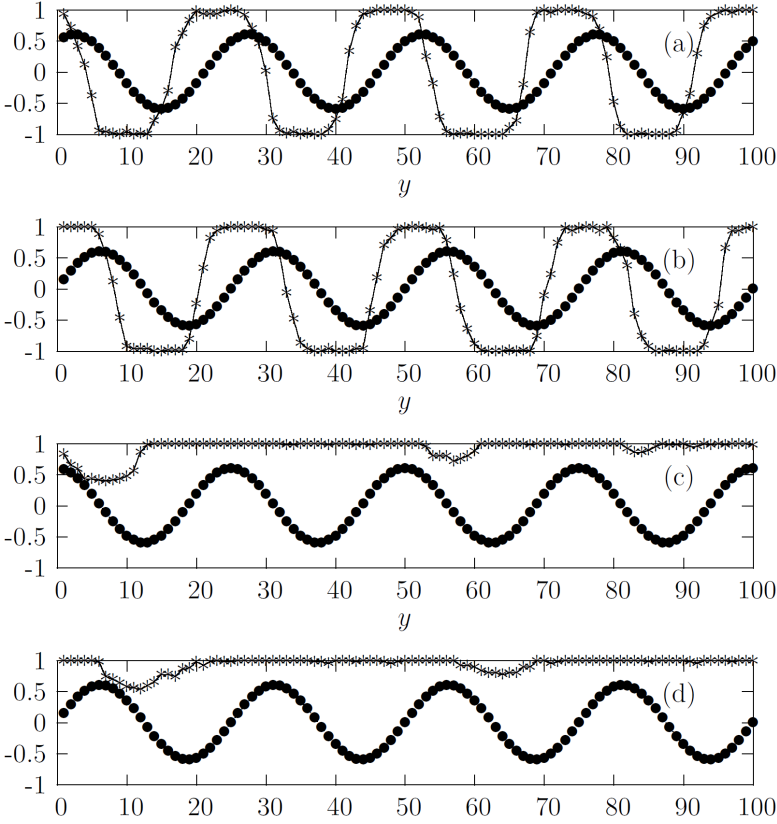


Fig. 2. The propagation of field ( $\bullet$ ) and the line magnetisation ( $*$ ) for various values of (a)  $t = 100100$  MCSS,  $T = 1.5$  and  $h_0 = 0.6$ , (b)  $t = 100125$  MCSS,  $T = 1.5$  and  $h_0 = 0.6$ , (c)  $t = 100100$  MCSS,  $T = 1.26$  and  $h_0 = 0.6$ , (d)  $t = 100125$  MCSS,  $T = 1.26$  and  $h_0 = 0.6$ .

The temperature variations of the dynamic order parameter  $Q$ , its variance  $\langle(\delta Q)^2\rangle$  are studied. The dynamic energy is  $E = f \oint H(t)dt$  and the dynamic specific heat is  $C = \frac{dE}{dT}$ . The derivatives are calculated numerically by using the three points central difference formula [24]. All these quantities are calculated statistically over 1000 different samples. The temperature variations of  $Q$ ,  $\frac{dQ}{dT}$ ,  $\langle(\delta Q)^2\rangle$  and  $C$  are studied for two different values of the amplitude of the propagating electromagnetic field wave and are shown in Fig. 3. As the temperature decreases,  $Q$  starts to grow from zero and near the transition point it becomes nonzero. Near the transition temperatures, the  $\langle(\delta Q)^2\rangle$  and  $C$  show sharp peak and  $\frac{dQ}{dT}$  show a sharp dip. From the figure, it is also evident that the transition occurs at lower temperature ( $T_d$ ) for higher values of the field amplitude ( $h_0$ ). In this case, for  $\lambda = 25$ , the transitions occur at  $T_d = 1.88$  and  $T_d = 1.29$  for  $h_0 = 0.3$

and  $h_0 = 0.6$  respectively. These values of the transition temperatures are obtained from the position of sharp dips of the  $\frac{dQ}{dT}$  and corresponding sharp peaks of  $\langle(\delta Q)^2\rangle$  and  $C$  shown in Fig. 3. Collecting all the values of the transition temperatures ( $T_d$ ) (depending on the values of  $h_0$ ), the comprehensive dynamical phase boundary is obtained.

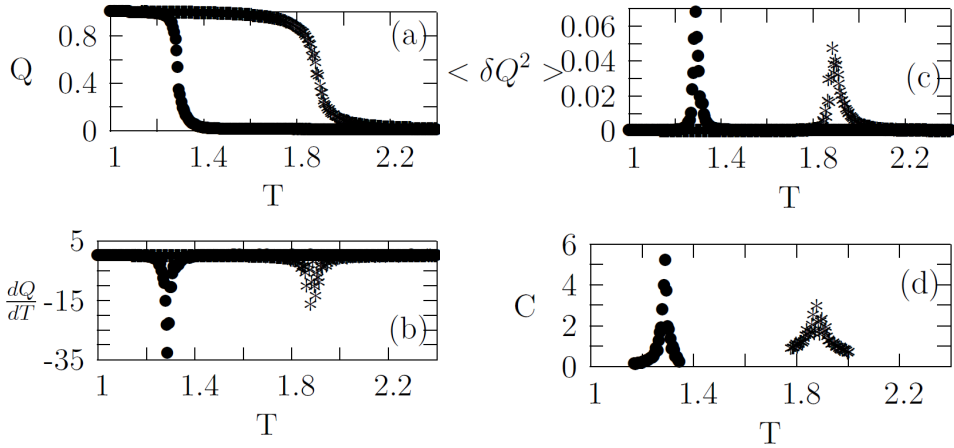


Fig. 3. The temperature ( $T$ ) dependences of the (a)  $Q$ , (b)  $\frac{dQ}{dT}$ , (c)  $\langle(\delta Q)^2\rangle$  and (d)  $C$ , for two different values of  $h_0$  for propagating magnetic field wave having  $f = 0.01$  and  $\lambda = 25$ . In each figure,  $h_0 = 0.3$ (\*) and  $h_0 = 0.6$ (•).

This dynamic transition temperature ( $T_d$ ) was observed to depend on the wave length ( $\lambda$ ) of the propagating magnetic field wave. The temperature dependences of  $Q$ ,  $\frac{dQ}{dT}$ ,  $\langle(\delta Q)^2\rangle$  and  $C$  are studied and shown in Fig. 4, for two different values of  $\lambda$  ( $= 25$  and  $50$ ). From the figure it is clear that transition occurs at higher temperature (with same  $h_0$ ) for higher value of the wavelength ( $\lambda$ ). To be precise, for  $h_0 = 0.3$ , the transitions occur at  $T_d = 1.88$  and  $T_d = 1.94$  for  $\lambda = 25$  and  $\lambda = 50$ , respectively. Here also, the values of the transition temperatures are obtained from the position of sharp dips of the  $\frac{dQ}{dT}$  and corresponding sharp peaks of  $\langle(\delta Q)^2\rangle$  and  $C$  (shown in Fig. 4). So, the dynamical phase boundary should shift depending on the value of  $\lambda$ .

In Fig. 5, the dynamical phase boundaries are drawn for two different values of  $\lambda$  ( $= 25$  and  $50$ ), in the plane formed by  $T_d$  and  $h_0$ . It is observed that the boundary shrinks inward (region of lower  $T$  and  $h_0$ ) as the wavelength of the propagating magnetic field decreases.

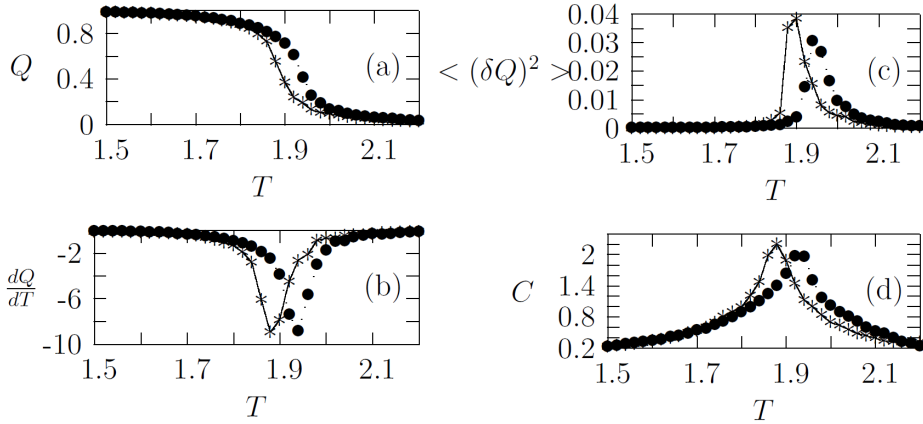


Fig. 4. The temperature ( $T$ ) dependences of the (a)  $Q$ , (b)  $\frac{dQ}{dT}$ , (c)  $\langle(\delta Q)^2\rangle$  and (d)  $C$ , for two different values of  $\lambda$  for *propagating* magnetic field wave having  $f = 0.01$  and  $h_0 = 0.3$ .

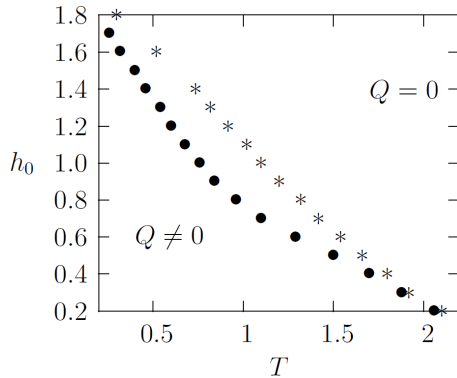


Fig. 5. The phase diagram for dynamic phase transition by propagating magnetic field wave for two different values of wavelengths,  $\lambda = 25(\bullet)$  and  $\lambda = 50(*)$ . Here,  $f = 0.01$ .

The dynamic phase transition, mentioned above, is associated with the divergences of relevant length scale. For this reason, the  $L^2\langle(\delta Q^2)\rangle$  is studied as the function of temperature  $T$ . It is found that the peak of  $L^2\langle(\delta Q^2)\rangle$  (observed at  $T_d$ ) increases as  $L$  increases. This is shown in Fig. 6. This result is quite conclusive to say that there exists the diverging length scale associated with the dynamic phase transition. It may be noted here that this method was successfully employed [4] to show the diverging length scale, associated with the dynamic transition, in the Ising ferromagnet driven by oscillating (but not propagating) magnetic field.

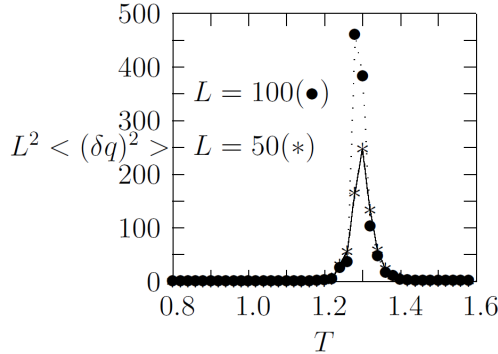


Fig. 6. The plot of temperature ( $T$ ) versus  $L^2\langle(\delta Q)^2\rangle$  for different system sizes ( $L$ ). Here,  $h_0 = 0.6$ ,  $\lambda = 25$  and  $f = 0.01$ .

#### 4. Summary

The dynamical responses of a ferromagnet to a polarised electromagnetic wave are modelled and studied here by the Monte Carlo simulation in the two-dimensional Ising ferromagnet. In the steady state, the coherent motion (in propagating mode) of spin clusters was observed. The time average magnetisation over the full cycle of the propagating EM wave is a measure of the order parameter in the dynamic phase transition observed here. The dynamic phase transition observed here seems to be of continuous type and found to be dependent on the amplitude and the wave length of the propagating polarised EM wave. Hence, a phase boundary (transition temperature as a function of the amplitude) is drawn for two different values of the wavelengths of EM wave. The phase boundary is found to shrink (towards the lower values of the temperature and amplitude of field) for shorter wavelength.

The signature of the divergence of relevant length scale near the transition is also observed here. This observation, in the case of dynamic transition, is analogous to that observed in equilibrium critical phenomenon revealing the growth of critical correlation. It would be interesting to know the universality class of this dynamic phase transition. To know the universality class, one has to estimate precisely the critical exponents, through a systematic study of scaling analysis.

The library facilities provided by the University of Calcutta is gratefully acknowledged.

## REFERENCES

- [1] B.K. Chakrabarti, M. Acharyya, *Rev. Mod. Phys.* **71**, 847 (1999); see also M. Acharyya, *Int. J. Mod. Phys.* **C16**, 1631 (2005).
- [2] M. Acharyya, B.K. Chakrabarti, *Phys. Rev.* **B52**, 6550 (1995); see also M. Acharyya, B.K. Chakrabarti, in: *Annual Reviews of Computational Physics*, Ed. D. Stauffer, World Scientific, Vol. 1, Singapore 1994, p. 107.
- [3] M. Acharyya, *Phys. Rev.* **E56**, 2407 (1997).
- [4] S.W. Sides, P.A. Rikvold, M.A. Novotny, *Phys. Rev. Lett.* **81**, 834 (1998).
- [5] M. Acharyya, *Phys. Rev.* **E59**, 218 (1999).
- [6] G. Korniss, P.A. Rikvold, M.A. Novotny, *Phys. Rev.* **E66**, 056127 (2002).
- [7] M. Acharyya, *Phys. Rev.* **E58**, 179 (1998).
- [8] H. Park, M. Pleimling, *Phys. Rev. Lett.* **109**, 175703 (2012).
- [9] O. Jiang, H.N. Yang, G.C. Wang, *Phys. Rev.* **B52**, 14911 (1995); Q. Jiang, H.N. Yang, G.C. Wang, *J. Appl. Phys.* **79**, 5122 (1996).
- [10] Y. Au *et al.*, *Phys. Rev. Lett.* **110**, 097201 (2013).
- [11] A. Berger *et al.*, *Phys. Rev. Lett.* **111**, 190602 (2013).
- [12] M. Acharyya, *Int. J. Mod. Phys.* **C14**, 49 (2003).
- [13] H. Jung, M.J. Grimson, C.K. Hall, *Phys. Rev.* **B67**, 094411 (2003).
- [14] H. Jung, M.J. Grimson, C.K. Hall, *Phys. Rev.* **E68**, 046115 (2003).
- [15] M. Acharyya, *Phys. Rev.* **E69**, 027105 (2004).
- [16] M. Keskin, O. Canko, B. Deviren, *Phys. Rev.* **E74**, 011110 (2006).
- [17] U. Temizer, E. Kantar, M. Keskin, O. Canko, *J. Magn. Magn. Mater.* **320**, 1787 (2008).
- [18] M. Acharyya, *J. Magn. Magn. Mater.* **323**, 2872 (2011).
- [19] M. Keskin, O. Canko, M. Kirak, *Phys. Stat. Solidi* **B244**, 3775 (2007); B. Deviren, M. Keskin, *Phys. Lett.* **A374**, 3119 (2010).
- [20] M. Acharyya, *Phys. Scr.* **84**, 035009 (2011).
- [21] M. Acharyya, *J. Magn. Magn. Mater.* **334**, 11 (2013).
- [22] M. Acharyya, *J. Magn. Magn. Mater.* **354**, 349 (2014).
- [23] K. Binder, D.W. Heermann, *Monte Carlo Simulation in Statistical Physics*, Springer Series in Solid State Sciences, Springer, New York 1997.
- [24] C.F. Gerald, P.O. Weatley, *Applied Numerical Analysis*, Reading, MA: Addison-Wesley, 2006; J.B. Scarborough, *Numerical Mathematical Analysis*, Oxford: IBH, 1930.